Combination of electrospray ionization, atmospheric pressure photoionization and laser desorption ionization Fourier transform ion cyclotronic resonance mass spectrometry for the investigation of complex mixtures - Application to the petroleomic analysis of bio-oils

Combination of electrospray ionization, atmospheric pressure photoionization and laser desorption ionization Fourier transform ion cyclotronic resonance mass spectrometry for the investigation of complex mixtures – Application to the petroleomic analysis of bio-oils

Jasmine Hertzog [1], Vincent Carré[1], Yann Le Brech[2], Colin Logan Mackay[3], Anthony Dufour[2], Ondřej Mašek[4], Frédéric Aubriet[1]

1 LCP-A2MC, FR 2843 Institut Jean Barriol de Chimie et Physique Moléculaires et Biomoléculaires, FR 3624 Réseau National de Spectrométrie de Masse FT-ICR à très haut champ, Université de Lorraine, ICPM, 1 boulevard Arago, 57078 Metz Cedex 03, France
2 LRGP, CNRS, Université de Lorraine, ENSIC, 1, Rue Grandville, 54000 Nancy, France
3 SIRCAMS, School of Chemistry, University of Edinburgh, Edinburgh, EH9 3FJ, Scotland, United Kingdom
4 UK Biochar Research Center, School of Geosciences, University of Edinburgh, Kings Buildings, Edinburgh, EH9 3JN, UK

Corresponding authors

Frédéric Aubriet

frederic.aubriet@univ-lorraine.fr

phone (33) 3 72 74 9 34
LCP–A2MC
ICPM,
1 boulevard Arago,
57078 Metz Cedex 03, France

Vincent Carré

vincent.carre@univ-lorraine.fr

phone (33) 3 72 74 9 33
LCP–A2MC
ICPM,
1 boulevard Arago,
57078 Metz Cedex 03, France

ABSTRACT

The comprehensive description of complex mixtures such as bio-oils is required to understand and improve the different processes involved during biological, environmental or industrial operation. In this context, we have to consider how different ionization sources can improve a non-targeted approach. Thus, the Fourier transform ion cyclotron resonance mass spectrometry (FT-ICR MS) has been coupled to electrospray ionization (ESI), laser desorption ionization (LDI) and atmospheric pressure photoionization (APPI) to characterize an oak pyrolysis bio-oil. Close to 90% of the all 4500 compound formulae has been attributed to $C_xH_yO_z$ with similar oxygen class compound distribution. Nevertheless, their relative abundance in respect with their double bound equivalent (DBE) value has evidenced significant differences depending on the ion source used. ESI has allowed compounds with low DBE but more oxygen atoms to be ionized. APPI has demonstrated the efficient ionization of less polar compounds (high DBE values and less oxygen atoms). The LDI behavior of bio-oils has been considered intermediate in terms of DBE and oxygen amounts but it has also been demonstrated that a significant part of the features are specifically detected by this ionization method. Thus, the complementarity of three different ionization sources has been successfully demonstrated for the exhaustive characterization by petroleomic approach of a complex mixture.

KEYWORDS

Non-targeted analysis, bio-oils, petroleomic approach, Ultra-high resolution mass spectrometry.

HIGHLIGHTS

- Non-targeted mass spectrometry approach by combining electrospray ionization, atmospheric pressure photoionization and laser/desorption ionization.
- Exhaustive description of pyrolytic bio-oil components.
- Distinction of sugaric derivatives, lignin derivatives and lipids contained in a woody-based pyrolytic bio-oil.

GRAPHICAL ABSTRACT

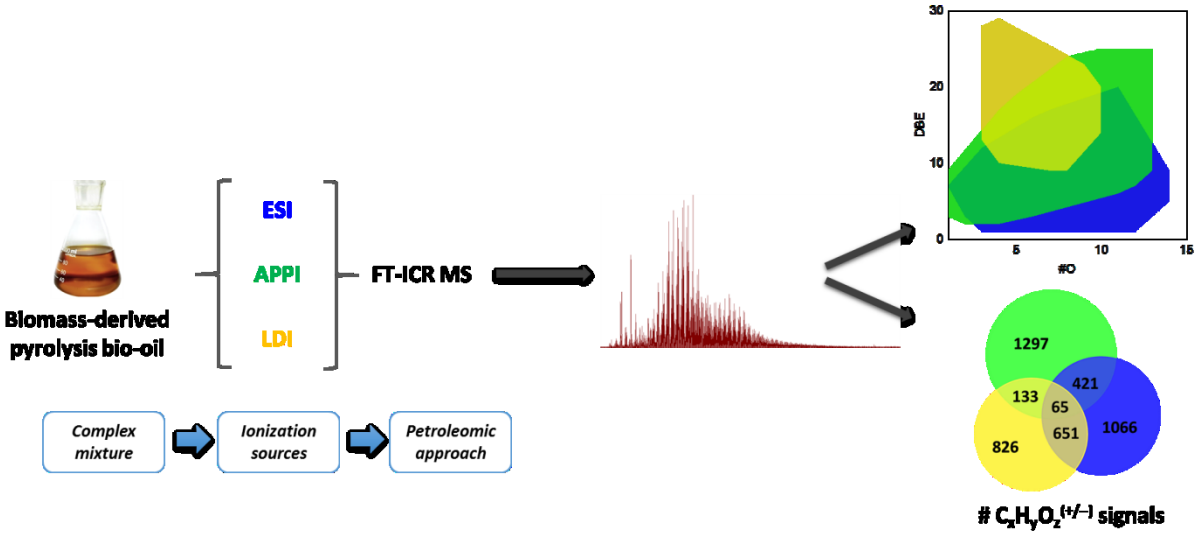

Color for online only

1. INTRODUCTION

The analysis of complex mixtures by mass spectrometry is currently still a challenge. Different methodologies may be used. The first category involves a targeted analysis using the combination of mass spectrometry with liquid or gas chromatography, which is limited to known class of compounds [1–4]. The second category, capable of a broader description of a complex mixture, includes non-targeted analysis methods, such as petroleomic or metabolomic approaches. Some works use gas or liquid chromatography [5,6], but the main part of non-targeted analyses in the field of petroleomic is performed without separation prior the acquisition of the mass spectrum. Therefore, it requires the use of ultra-high mass resolution and accurate mass measurement analysis due to the absence of separation prior the acquisition of the mass spectrum. Fourier transform ion cyclotron resonance mass spectrometry (FT-ICR MS) [7–11] and in a lesser extent the Fourier transform Orbitrap mass spectrometry (FT-Orbitrap MS) [12–14] represent techniques from the second category. These techniques offer numerous advantages as an exhaustive description of complex mixtures and the reduced time of data acquisition, but also suffer from several drawbacks. The key obstacle in non-target analysis is the ionization competition effect, which ensures the detection of easy ionized species (not always the most abundant) at the expense of other mixture components. The combination of different ionization techniques such as electrospray (ESI), laser desorption (LDI) and atmospheric pressure photoionization (APPI) as well as the analysis of positive and negative ions may overcome this problem [15–17].

Pyrolysis bio-oil is a good example of a highly complex mixture made up of thousands of compounds with differing properties [18]. Furthermore, their composition changes depending on the raw feedstocks and the conditions employed for their production and/or the catalytic treatment carried out prior to their use as bio-fuel [19,20]. Indeed, pyrolysis bio-oil components are too oxygenated to allow their direct use as a fuel and require catalytic treatment to remove the main part of the oxygen atoms. Exhaustive and accurate characterization is required to improve, the pyrolysis process itself and the catalytic treatment efficiency [21–24]. This can be achieved through application of the petroleomic non-targeted approach with FT-ICR MS [25–27] or FT-Orbitrap MS [28,29], whereby a part of the total composition of bio-oil can be elucidated.

The majority of published studies dealing with the characterization of pyrolysis bio-oils by FT-ICR MS were conducted using ESI typically in negative ion mode. Different sample preparations (with or without fractionation of the sample) or the addition of dopant to increase the ionization yield have been reported. Miettinen *et al.* [30] and Jarvis *et al.* [31] have analyzed the aqueous and oily phases of different pyrolysis bio-oil after fractionation. In both studies, the heteroatom class distributions showed larger amounts of highly oxygenated compounds in the aqueous fraction than in the oily

phase. The authors concluded that the aqueous phase is mainly composed of "sugaric species"; whereas the oily phase is composed of lipids and pyrolytic lignin derivatives. A more exhaustive fractionation method was used by Liu *et al.* [32] to fully characterize by (–) ESI FT-ICR MS the pyrolytic bio-oil of red pine. The least polar fractions of bio-oil were not ionized when the raw bio-oil was infused in the ESI source due to ionization extinction effect. We recently proposed the use of different dopants to improve ionization efficiency in (+/–) ESI FT-ICR MS [33]. In that case, it was possible to detect on the same mass spectrum, without fractionation, the bio-oil components of the aqueous and oily phases. The effect of alternative dopants in (–) ESI FT-ICR MS has been demonstrated to improve deprotonation (addition of NH_4OH [15,25,26] or NaOH [15]) or to favor the formation of $[M+Cl]^-$ adduct ion (NH_4Cl dopant) [15]. In (+) ESI FT-ICR MS, formic acid and NH_4Cl (formation of $[M+H]^+$) or NaCl (generation of $[M+Na]^+$ sodiated ion) ions have been used [15]. Regardless of these advances, ESI exhibits poor ionization of non-polar compounds. The use of LDI or APPI has been previously proposed to detect these non- or poorly-ionized bio-oil components.

Cole *et al.* [28] investigated nitrogen species from raw switch grass pyrolysis bio-oils using ESI and APPI FT-Orbitrap MS and have shown that N_1 and N_2 compounds are the dominant species observed with (+) ESI FT-Orbitrap MS whereas with (+) APPI FT-Orbitrap MS the majority were oxygen-containing species. They also characterized the less complex toluene extracts from biochar by FT-Orbitrap MS with ESI, APPI and LDI sources [17]. Leonadis *et al.* [34] investigated the less polar bio-oil components (aromatic and aliphatic carbon and nitrogen-containing species) by APPI FT-ICR MS. More recently, Chiaberge *et al.* [10] demonstrated the ability of APCI and APPI FT-ICR MS to detect less polar and apolar bio-oil components whereas ESI FT-ICR MS is more suited for polar species. We have also demonstrated the capability of combining LDI FT-ICR MS and ESI FT-ICR MS analysis to investigate raw or HDO-treated lignin pyrolysis bio-oils [23].

Overall, the literature demonstrates that to attain a complete description of a complex mixture, such as bio-oil, complementary ionization techniques must be used. In this study a comprehensive investigation of one complex mixture, an oak pyrolysis bio-oil, was performed using ESI, LDI and APPI. This is the first time such a detailed petroleomic study has been conducted for bio-oil.

2. MATERIALS AND METHODS

2.1. Bio-oil production

The bio-oil was produced by pyrolysis in a micro-fluidized bed reactor set at 500 °C (temperature of the sand) for 12 min. Two grams of oak powder were continuously injected in to the bed *via* a micro-feeder developed at CNRS Nancy. More details about the process and the raw

material composition are available in previous work [35]. The bio-oil was recovered in methanol (the "bio-oil solution") and stored at –20°C, prior to analysis.

2.2. Preparation of the samples

LCMS grade methanol (VWR−Prolabo), water (Fisher Chemical), and sodium acetate (Fisher Scientific) were used as supplied. For the ESI FT-ICR MS analyses, the bio-oil was diluted to a final concentration of 2% in methanol. Sodium acetate (0.1 $mg.mL^{-1}$) was added to favor cationization [33]. For the APPI experiments, the sample is diluted in methanol (4% v/v) without addition of dopant. For LDI experiments, 1 µL of bio-oil/water (70% v/v) solution was deposited on a stainless steel target and dried at room temperature.

2.3. Fourier Transform Ion Cyclotron Resonance Mass Spectrometers

The instrument used for the analyses was a 12 T SolariX FT-ICR equipped with ESI, APPI and LDI sources (Bruker Daltonics). The different ionization methods and operating parameters were optimized via the FTMSControl V2.1.0, build 98 (Bruker Daltonics). Alternatively, some LDI FT-ICR MS measurements were performed on a 9.4 T IonSpec active shielded mass spectrometer.

2.3.1. ESI FT-ICR MS

ESI FT-ICR MS analyses were performed in both positive and negative ion modes. The capillary voltage was set at ± 4000 V and the end plate offset at – 500 V. The source gas was tuned with nebulizer gas (1 – 1.8 bar), dry gas (4 – 6 L/min) and heated at 180 °C. The sample was infused at a flow rate of 200 $\mu L.h^{-1}$ into the ion source. The ions were accumulated for 0.3 s per scan and 200 analyses were summed to obtain the final mass spectrum in the 129 to 1000 *m/z* range. The length of the transient was 3 s and the mass resolution was ≈680 000 at *m/z* 400.

2.3.2. APPI FT-ICR MS

The analyses were performed in positive ion mode with the APPI source equipped with a krypton lamp at 10.6 eV. The voltages of the capillary and the end plate were set at ± 1000 V and – 500 V, respectively. The nebulizer and dry gas were tuned at 1.8 bar and 6 $L.min^{-1}$ respectively and the source heated to 180 °C. The sample was infused at a flow rate of 1 $mL.h^{-1}$ and the ions were accumulated for 0.05 s. The mass spectra acquired in the 129 to 1000 *m/z* range were the sum of 100 analyses. The transient length was 1.5 s and the mass resolution was ≈340 000 at *m/z* 400.

2.3.3. LDI FT-ICR MS

The measurements were performed in negative ion mode. Fifty analyses were accumulated to obtain the final mass spectrum in the 147 to 1000 *m/z* range. Measurements were conducted at

the 355 nm wavelength with a diameter of the laser spot of 300 µm. Six hundred laser shots per analysis were accumulated at a 1000 Hz laser frequency. A 1.7s transient length was acquired, which resulted in mass resolution of ≈390 000 at *m/z* 400. The power of the laser was optimized to avoid fragmentation and recombination phenomenon [36].

Other experiments were performed using a 9.4 T LDI FT-ICR mass spectrometer (IonSpec, Lake Forest, CA). LDI was performed by a Nd:YAG ORION air-cooled laser system (New Wave Research Inc, Fremont, CA) working at 355 nm.

The laser power was kept down to 0.7 J cm^{-2} to avoid fragmentation processes and to obtain intense ion signals. A decrease of the laser power did not modify the nature of the detected species but induced a significant decrease in their abundance. The resulting ions from (8 laser shots) were stored in a RF-only hexapole before their transfer to the FT-ICR cell. The ion guide was tuned to optimize the efficient transfer of ions in the *m/z* 150−500 range into the FT-ICR MS cell. A 1.049 s transient length was acquired with 4096 K data points. Typically, the average mass measurement accuracy was better than 500 ppb, and the mass resolution was between 500 000 and 2 000 000. To increase the signal to noise ratio, each mass spectrum reported in following sections was the sum of 45 individual mass spectra.

2.4. Data post-acquisition treatment

The ESI/LDI and APPI FT-ICR MS mass spectra (**S.I. 1 and S.I. 2)** were analyzed using Data Analysis V4.4, build 102.47.2299 (Bruker Daltonics) and calibrated with well-known oxygenated compounds and a peak list, for each mass spectrum, was generated for all ions with a S/N ratio greater than 4. PetroOrg software (Florida State University) was used for the peak assignment. The attribution parameters were set as following: $C_{1\text{-}100}H_{2\text{-}200}O_{1\text{-}20}N_{0\text{-}20}S_{0\text{-}1}$ (for negative ion mode). Sodium adducts are considered for (+) ESI analyses. The tolerated mass error was ± 1 ppm. The identified peaks and the efficiency of the calibration was checked by the graph representing the mass error against *m/z* (**S.I. 3**) and the value of the RMS.

For 9.4 T LDI FT-ICR MS measurements prior to acquisition, the mass spectrometer was externally calibrated by considering well-known ions such as hydride gold cluster ions. Following acquisition, internal calibration was performed with specific and well characterized $C_xH_yO_{3,4,5}^{+/-}$ ion series. A peak list of signals with a S/N > 4.5 was generated and the Composer software (Sierra Analytics, Modesto, CA) was used for ion assignment with the following search criteria: $C_{1–100}H_{1–100}N_{0–5}O_{0–30}Na_{0–1}^{+}$ (positive ion) or $C_{1–100}H_{1–100}N_{0–2}O_{1–30}S_{0–1}^{-}$ (negative ion) general formula, 3 ppm tolerance error, and a double bound equivalent (DBE) ranging from 0 to 40. The recalibration of the mass spectrum was then conducted with signals assigned with an error lower than 1 ppm by considering

the following equation with m/z the mass-to-charge ratio, m (uma) the mass and z the charge of the ion, f the measured frequency (Hz) and, A and B the constraints:

$$\frac{m}{z} = \frac{A}{f} + \frac{B}{f^2}$$

For the non-assigned signals or the assigned signals with an error greater than 1 ppm a manual assignment was conducted by using Omega 8 Elemental Composition software (Varian-IonSpec Inc.) with the previously reported search criteria.

Post-treatment was applied to process data to achieve some graphical representations that were necessary in order to compare the results obtained in the different analytical conditions. More specifically, van Krevelen diagrams were used to illustrate the different components of the bio-oil. Each compound was represented by a dot where the x and y coordinate represent its O/C and H/C ratio, respectively. This representation ensures to distinguish species which are relative to lipids (low O/C ratio and H/C ratio close to 2), sugaric derivatives (high O/C and H/C ratios) and pyrolytic products of the lignin (H/C value close to 1 and O/C ratio in the 0.2 to 0.6 range) (**S.I. 4**)

3. RESULTS AND DISCUSSION

3.1. ESI FT-ICR MS

Whatever the ion detection mode, 95% of the signal is attributed to $C_xH_yO_z$ compounds (**Table 1**), the composition of which is consistent with the elemental analyses of oak bio-oil [35]. In (+) ESI, the remaining signal is attributed to $C_xH_yNO_z$ compounds whereas in (–) ESI, both $C_xH_yNO_z$ and $C_xH_ySO_z$ species are identified and correspond to 2% and 3% of the total ion signal, respectively. In (+) ESI, NO_z ions are detected as $[M+H]^+$, which corresponds to protonation of the basic sites of the molecule such as amine group or pyridine ring [28]. This is in agreement with the dramatically increase of the signals attributed to nitrogen-containing species when formic acid is added to the sample [33]. NO_z anions are thought to be related to neutral or acidic compounds, which may include for example an indole moiety. It is proposed that the SO_z species are associated with aromatic sulfonated compounds, which easily deprotonate. Alternatively, they may also correspond to HSO_4^- attachment to $C_xH_yO_z$ bio-oil components during the ESI process [37]. The $[M–H]^-$ anion and the $[M+Na]^+$ cation distribution of the $C_xH_yO_z$ bio-oil components present similarities in terms of DBE and the number of oxygen atoms. Nevertheless, differences are highlighted when the relative intensity of these compounds is considered (**Figure 1**). In (–) ESI, the $[M–H]^-$ ions illustrate a wide variation in the number of oxygen atoms (O2 to O16). The most important signal is observed for O4 to O6 compounds. Sodiated cations $[M+Na]^+$ are detected for O1 to O14 bio-oil components, the most abundant signal is obtained for O5 and O6 species and, a bimodal distribution is observed. The second massif is centered on O11 compounds. This behavior has been observed in a previously

published work dealing with the study of Miscanthus bio-oil by ESI FT-ICR MS under similar experimental conditions [33]. Furthermore, the van Krevelen diagrams of $C_xH_yO_z$ compounds detected in (–) ESI and (+) ESI are reported in **Figure 2**. Lipids are predominantly observed in (–) ESI but are also observed in (+) ESI. In both ion detection modes, the pyrolytic lignin derivatives constitute the majority of the signal. Nevertheless, (–) ESI analysis reveals a more extended distribution of compounds in terms of unsaturation number and oxygen amounts. The sugaric compounds are more numerous and abundant in (+) ESI. The ability of highly oxygenated compounds to easily poly-coordinated the sodium cation explains this behavior.

It has to be noted that these results display significant similarities with the works of Miettinen *et al.* [30] and Jarvis *et al.* [31] who investigated by (–) ESI FT-ICR MS after fractionation the oily and aqueous phases from different pyrolysis bio-oils. Lipids and pyrolytic lignin derivatives were common to both fractions whereas "sugaric species", which correspond to the most oxygenated compounds, were only highlighted in the aqueous phase. These latter compounds are relative to the second distribution (centered on O11) observed in this study for $[M+Na]^+$ ions. The first massif of the O-containing bio-oil components, common to both ion detection modes, is indicative of the pyrolytic lignin derivatives. In spite of a lower sensitivity of (+) ESI for pyrolytic lignin derivatives and lipids, it is the only experimental condition able to give semi-quantitative information regarding the sugaric and lignin pyrolysis compounds. As a conclusion, both detection modes are useful for the thorough characterization of bio-oil.

The comparison of the obtained results with previously published works [15,38,39] can be made to tentatively assign some signals, obtained by (+) or (–) ESI FT-ICR MS (see S.I. 2a and 2b), to well-known pyrolysis compounds derived from the wood constituents. Thus, the ions observed at *m/z* 185.04213, 187.05764 and 347.09467 may be attributed to $[M + Na]^+$ adducts of levoglucosan, glucose and cellobiosan, which are cellulose and hemi-cellulose pyrolysis products. The specific compounds, which derivate from the lignin pyrolysis may also be observed in the form of $[M + Na]^+$ and/or $[M – H]^–$. Cinnamic acid and coniferyl aldehyde, two of the lignin paracoumaryl unit derivate are detected as $[M – H]^–$ ion at m/z 147.04512 and 177.05571,respectively. Pyrolysis compounds of guaiacyl (vanillin, eugenol, acetoguaiacon), and syringyl (syringol, methylsyringol, syringaldehyde) units were also evidenced (see S.I.3)

3.2. APPI FT-ICR MS

The predominant part of the total ion current (TIC) observed in (+) APPI, is the results of O-containing compounds. The NO_z species only represents 10% of the signal. The O_z-species distribution ranges from O1 to O13 with maxima around O6-O7 (**Figure 1**). The corresponding van

Krevelen diagram (**Figure 2**) indicates that both lipids and pyrolytic lignin derivatives are observed in APPI. In spite of limited reported data on APPI analyses of woody bio-oils, the comparison with Osborne *et al.* [40] investigation of dissolved organic nitrogen-containing compounds by APPI FT-ICR MS demonstrates that neither proteins nor tannins are detected by (+) APPI FT-ICR MS of pyrolysis bio-oils. As we observed, only lignin derivate compounds and lipids but not cellulose-linked species are detected. Thus, APPI should be considered as inefficient for the ionization of sugaric derivatives.

Further examination of (+) APPI mass spectrum, reveals that 75 % of the TIC for O-containing bio-oil components is associated with protonated species and the other species are molecular $M^{\bullet+}$ ions. Different ionization pathways may explain the formation of the observed cations, considering that no dopant was added in our (+) APPI experiments. Due to the ionization energy of methanol (10.84 eV), the solvent cannot be directly photoionized by Kr photons (10.6 eV), but the dimer of methanol, corresponding to 2% of the methanol in solution, has a lower ionization energy (9.74 eV) and is efficiently ionized [41]. The radical cation dimer may yield a protonated methanol ion by elimination of a $CH_3O^{\bullet}$ (or $^{\bullet}CH_2OH$) radical. Additionally, the generation of large protonated methanol clusters is facilitated by the large binding energy of neutral CH_3OH to protonate solvent clusters, e.g., CH_3OH binding energy with $[CH_3OH]_nH^+$ is – 33 kcal/mol for n = 1, – 22 kcal/mol for n = 2, and – 16 kcal/mol for n = 3 [42]. The interaction of these protonated methanol clusters with O-containing bio-oil components induces the transfer of the proton, and eventually the fission of the methanol cluster, to the most acidic bio-oil compounds. Wood pyrolysis bio-oils typically have a low pH values and significant amounts of acidic compounds [20]. More specifically, this happens for O/C > 0.4 compounds, which have odd *m/z* values (**S.I 5**). The formation of even *m/z* ions may be the result of the direct photoionization, according low ionization energy of highly unsaturated and conjugated species or charge transfer from the $[CH_3OH]_2^{\bullet+}$ ion. Alternatively, part of the large number of the bio-oil components may act as a self-dopant. It has to be noted that the addition of a typical APPI dopant (toluene) had no significant effect on the obtained mass spectrum.

3.3. LDI FT-ICR MS

The experiments were conducted in both positive and negative mode. In this latter case, both 9.4 T and 12 T instruments were used. The majority of detected ions are O-containing compounds, independent of the instrument or the ion detection mode used. This observation is more pronounced in negative LDI FT-ICR MS for which the obtained distribution with the 12 T instrument is $C_xH_yO_z$ (92 %), $C_xH_yNO_z$ (3%) and $C_xH_ySO_z$ (5%) and $C_xH_yO_z$ (97 %), $C_xH_yNO_z$ (3%) and $C_xH_ySO_z$ (0.3%) for the 9.4 T FT-ICR mass spectrometer (**Table 1**). The distribution of O-containing species presents a maximum at O6 components in negative ion detection mode. A broad distribution of the number of oxygen atoms is observed for the 12 T instrument (from O3 to O17); whereas the

mass spectrum obtained with the 9.4 T mass spectrometer limits the distribution to 10 oxygen atoms. In (+) LDI, the signal is relative to $C_xH_yO_z$ (83% of the TIC) and $C_xH_yNO_z$ (17% of the TIC) compounds. The O-containing compounds ranges from O2 to O14 with maxima observed for O4 – O5 species (**Figure 1**). The species containing 8 to 14 oxygen atoms are detected as sodium adducts. These sodium ions originate from the solvents used in the analysis. In gas phase, Na^+ easily coordinates with low unsaturated compounds which contain a significant amount of oxygen atoms.

According to the O/C and H/C ratios, both pyrolytic lignin derivatives and sugaric compounds (but not lipids) are detected on the 12 T (–) LDI mass spectrum (**Figure 2**). The 9.4 T (–) LDI, leads to the specific observation of the pyrolytic lignin compounds (**Figure 2**). Lignin linked compounds are observed in the LDI experiments due to their significant absorption properties at the laser wavelength used. This is confirmed by previous work carried out by Olcese *et al.* [23] who investigated bio-oils produced by pyrolysis of lignin for which O2 to O8 compounds with DBE values ranging from 7 to 25 were observed. Smith *et al.* [29] also observed that O4, O5 and O6 were the main O-containing bio-oil component observed by LDI–Orbitrap MS. Differences in (–) LDI results obtained with the 12 T and 9.4 T instruments can be explained with the different 355 nm laser profiles of both setups. The energy surface distribution of the smartbeam™ laser which is coupled with the 12 T FT-ICR MS instrument is less homogeneous than the Orion. Indeed, the "average homogeneity" of the smartbeam™ is obtained by the repetition on the same area of a large number of different laser shots [43]. For the Orion laser, each laser shot is more homogeneous. As a consequence, the smartbeam laser leads to the formation of hot (and cold) spots, for which the laser energy may be higher (and lower) than the laser energy deposited at the surface of the sample by the Orion laser. Typically, the compounds which have low absorption properties (in this case sugaric compounds) need high laser energy to be desorbed and ionized. Such conditions occur in the hot spots of the smartbeam™ laser but not with the homogeneous Orion laser.

In LDI, compounds are detected as radical or protonated/deprotonated ions. The radicals are highly unsaturated compounds (H/C < 1) with O/C < 0.4, as shown in **S.I. 5**. Among the O-containing species, only 4% of the signal is attributed to $M^{\bullet-}$ ions using the 12 T mass spectrometer (**S.I. 4**). Whereas, when using the 9.4 T equipped with the Orion laser, they represent 22% ($M^{\bullet+}$) and 15% ($M^{\bullet-}$). It is proposed that these differences are linked to the laser-sample interaction which is strongly dependent on the laser beam as previously mentioned.

3.4. Complementarity of the different ionization sources

Irrespective of the ionization method used and the ion detection mode, the obtained compound class distribution is mainly associated with O-contained compounds, which is consistent with CHNOS elemental analysis, at least 90% of the TIC is related to $C_xH_yO_z$ compounds (**Table 1**).

Nitrogen species are always detected while SO_z compounds are only detected in negative ion detection mode. **Figures 2 and 3** well illustrate the complexity of the bio-oil samples and the complementarity of ESI, APPI and LDI sources for their ionization and analysis.

3.4.1. Positive ion mode analyses

The distributions of the O-species achieved in (+) ESI and (+) APPI appear very similar based on the importance of O_z bio-oil components (**Table 1**), which extend to a similar range from O1 to O14 and from O1 to O13, respectively. However, further insight can be gained by assessing the intensity of the DBE distribution for each heteroatom class (**Figure 1**). In ESI, the most intense compounds detected contain 10 and 11 oxygen atoms and have DBE < 5. The other prominent species are composed of 5 to 7 oxygen atoms and their DBE values range from 0 to 5. The most oxygenated species have the properties of pyrolytic sugaric derivatives whereas the less oxygenated ones are pyrolytic lignin derivatives and lipids, these components were also evidenced on a Miscanthus bio-oil in (+) ESI [33]. On the other hand, in case of APPI, compounds having 10 or more oxygen atoms are not significant which means that sugaric compounds are not ionized in APPI. However, species containing 4 to 8 oxygen atoms are intensely detected, which is also seen using ESI. But their unsaturation degree is much more important, with DBE ranging between 5 and 20. These molecular properties can be attributed to pyrolytic lignin derivatives and lipids. Moreover, compounds identified in ESI contain up to 30 carbon atoms on a mass range of *m/z* 150 to 600 whereas in APPI, they have up to 40 carbon atoms and a mass range from *m/z* 200 to 800.

Thus, APPI is useful to observe the highest mass-to-charge-ratio compounds with high DBE values and low polarity (not observed on (+) ESI mass spectrum). Nevertheless, these hetero-polyaromatic compounds are not totally apolar due to their capability to be ionized in APPI by protonation rather than charge transfer. ESI is a suitable method to observe polar to middle polar compounds which are characterized by a low unsaturation degree and a significant amount of heteroatoms such as oxygen in the case of bio-oils [10,13,16]. The (+) LDI analysis yields results very similar to those obtained by (+) ESI and (+) APPI. It leads to an intermediate behavior and allows both middle polar to low polar bio-oil components to be observed at the exception of the high mass species. The combination of the different used ionization methods is consequently well suited to exhaustively describe pyrolytic bio-oil.

The examination of the obtained signals in respect to the DBE value and the number of oxygen atoms for the three different ionization techniques **Figure 1** highlights that positive ESI is more sensitive to ionization competition. More specifically, highly saturated compounds with high levels of oxygen are well suited to form stable sodium adducts which lead to the increase of the associated signal. The same kind of discrimination is observed with components presenting a high

proton affinity when bio-oil is directly infused in the ESI source. In contrast, positive APPI and in a lesser extent positive LDI lead to a less compound-dependent ionization and ensure a more precise description of the bio-oil component distribution to be obtained but only on pyrolytic lignin species.

3.4.2. Negative ion mode analyses

The $C_xH_yO_z$ compound distributions obtained in (–) ESI and (–) LDI are very similar in respect with the oxygen atom amounts (**Figure 1**). In both ionization modes, a broad O-class of compounds are detected, with O2-O16 components in (–) ESI and O3-O17, in (–) LDI using the 12 T FT-ICR MS. The O-species range obtained with the 9.4 T FT-ICR MS is narrower (O3 to O10 oxygen atoms). However, when using either instrument, the O4 to O6 species are the most predominant. These observed trends are very similar to those obtained in positive detection mode with ESI, LDI and APPI. As shown in **Figure 1**, degree of unsaturation is more important for compounds detected in LDI than those in ESI. These results are consistent with published literature. For example, the LDI and ESI analyses of extracts from fast pyrolysis char obtained by Cole *et al.* [17] present similar distribution of compounds in respect to their heteroatom classes with a DBE distribution centered at higher values in LDI. Consequently, this behavior has to be considered as a generalization for woody bio-oils of what we previously reported for lignin pyrolysis products [23]. Thus, negative LDI exhibits the capability to efficiently ionize low to medium polar compounds presenting different amounts of oxygen atoms and a high number of unsaturation, which is due to the absorption properties at the wavelength of the ionization laser, whereas negative ESI is more suited to more polar species such as lipids.

The comparison of positive and negative mode van Krevelen diagrams for lignin derivate compounds is also of significant interest. The O/C ratio is very similar and generally ranges from 0.1 to 0.7. In contrast, the H/C ratio varies significantly. For LDI and APPI, this ratio for the observed compounds is centered on 1, in contrast it is significantly higher in positive ESI and lower in negative ESI. ESI ensures the efficient ionization of polar compounds, positive ESI is sensitive to basic compounds whereas negative ESI is well suited to neutral or acidic species. APPI and LDI are less sensitive to these differences in chemical properties and as a consequence, the acidic and neutral fraction of bio-oil is predominantly highly unsaturated species, which easily deprotonated to produce anions stabilized by significant mesomeric effects.

The complementarity of the ionization sources is also assessed by the Venn diagrams giving the repartition of the different 4500 compound formulae depending on the ionization source and the ion polarity (**Figure 3**). In positive ion mode (**Figure 3a**), APPI enabled to identify 1297 exclusive formulae whereas ESI and LDI allowed to attribute 449 and 92 own formulae, respectively. As a result, only 65 compounds were common to the 3 ionization sources. Besides, the same

representation was done in negative ion mode (**Figure 3b**), with ESI and LDI. It appeared that 617 formulae were specific to ESI, and 625 to LDI in the best conditions. Finally, as (−) ESI has been the only ionization method in most bio-oil analyses [22], it is clearly demonstrated here that this strategy nearly highlights 1250/4500 elemental formulae corresponding to less than 28% of the total bio-oil components.

4. CONCLUDING REMARKS

Comprehensive petroleomic analysis of bio-oil by ESI, APPI and LDI FT-ICR MS, showed that the heteroatom distributions as obtained by these three different methods were very similar. In fact, for any given ion detection mode, the $C_xH_yO_z$ species are the most abundant compound family and their distributions extend across comparable ranges of oxygen atom numbers. However, when focused on the DBE distributions obtained for each of the ionization modes, some differences became apparent. In ESI, the compounds were more highly saturated, with $2 < DBE < 10$, whereas in APPI, they were more unsaturated with $5 < DBE < 20$. In LDI, the range of unsaturation was between those obtained by ESI and APPI but it was also affected by the FT-ICR MS laser configuration. With a non-homogeneous laser beam, components identified were less unsaturated

This approach successfully demonstrated that the characterization of complex mixtures by non-targeted analysis required the use of different but complementary ionization sources in order to have the most exhaustive as possible description. Indeed, at the maximum, the common used negative ESI only allowed the MS detection of less than 28% of the combined features obtained by ESI, APPI and LDI FT-ICR MS.

ACKNOWLEDGMENTS

The authors, more especially Jasmine Hertzog, would like to thank the European COST Action 1306 “Lignoval” for its financial support, as it enabled a new collaboration between the LCP-A2MC, Université de Lorraine and the UK Biochar Research Center, Edinburgh University. The analyses with the 9.4 T FT-ICR MS where performed at the LCP-A2MC whereas the measurements carried out with the 12 T FT-ICR MS were done at the Scottish Instrumentation and Resource Centre for Advanced Mass Spectrometry (SIRCAMS) at the University of Edinburgh. The TGIR program FR 3624, infrastructure program of CNRS, is acknowledged for further financial support. Authors also thank Dr Faye Cruickshank for her valuable editing of the manuscript.

REFERENCES

[1] P.M. Medeiros, B.R.T. Simoneit, Analysis of sugars in environmental samples by gas chromatography–mass spectrometry, J. Chromatogr. A. 1141 (2007) 271–278. doi:10.1016/j.chroma.2006.12.017.

[2] Y.S. Choi, P.A. Johnston, R.C. Brown, B.H. Shanks, K.-H. Lee, Detailed characterization of red oak-derived pyrolysis oil: Integrated use of GC, HPLC, IC, GPC and Karl-Fischer, J. Anal. Appl. Pyrolysis. 110 (2014) 147–154. doi:10.1016/j.jaap.2014.08.016.

[3] P. Jonsson, A.I. Johansson, J. Gullberg, J. Trygg, J. A, B. Grung, S. Marklund, M. Sjöström, H. Antti, T. Moritz, High-Throughput Data Analysis for Detecting and Identifying Differences between Samples in GC/MS-Based Metabolomic Analyses, Anal. Chem. 77 (2005) 5635–5642. doi:10.1021/ac050601e.

[4] J. Peng, J.E. Elias, C.C. Thoreen, L.J. Licklider, S.P. Gygi, Evaluation of Multidimensional Chromatography Coupled with Tandem Mass Spectrometry (LC/LC−MS/MS) for Large-Scale Protein Analysis: The Yeast Proteome, J. Proteome Res. 2 (2003) 43–50. doi:10.1021/pr025556v.

[5] K. Fraser, S.J. Harrison, G.A. Lane, D.E. Otter, Y. Hemar, S.-Y. Quek, S. Rasmussen, Non-targeted analysis of tea by hydrophilic interaction liquid chromatography and high resolution mass spectrometry, Food Chem. 134 (2012) 1616–1623. doi:10.1016/j.foodchem.2012.03.045.

[6] K. Hanhineva, I. Rogachev, H. Kokko, S. Mintz-Oron, I. Venger, S. Kärenlampi, A. Aharoni, Non-targeted analysis of spatial metabolite composition in strawberry (Fragaria × ananassa) flowers, Phytochemistry. 69 (2008) 2463–2481. doi:10.1016/j.phytochem.2008.07.009.

[7] J.S. Sampson, A.M. Hawkridge, D.C. Muddiman, Generation and Detection of Multiply-Charged Peptides and Proteins by Matrix-Assisted Laser Desorption Electrospray Ionization (MALDESI) Fourier Transform Ion Cyclotron Resonance Mass Spectrometry, J. Am. Soc. Mass Spectrom. 17 (2006) 1712–1716. doi:10.1016/j.jasms.2006.08.003.

[8] C.A. Hughey, R.P. Rodgers, A.G. Marshall, Resolution of 11 000 Compositionally Distinct Components in a Single Electrospray Ionization Fourier Transform Ion Cyclotron Resonance Mass Spectrum of Crude Oil, Anal. Chem. 74 (2002) 4145–4149. doi:10.1021/ac020146b.

[9] D. Cao, H. Huang, M. Hu, L. Cui, F. Geng, Z. Rao, H. Niu, Y. Cai, Y. Kang, Comprehensive characterization of natural organic matter by MALDI- and ESI-Fourier transform ion cyclotron resonance mass spectrometry, Anal. Chim. Acta. 866 (2015) 48–58. doi:10.1016/j.aca.2015.01.051.

[10] S. Chiaberge, I. Leonardis, T. Fiorani, P. Cesti, S. Reale, F. De Angelis, Bio-Oil from Waste: A Comprehensive Analytical Study by Soft-Ionization FTICR Mass Spectrometry, Energy Fuels. 28 (2014) 2019–2026. doi:10.1021/ef402452f.

[11] A.G. Marshall, R.P. Rodgers, Petroleomics: The Next Grand Challenge for Chemical Analysis, Acc. Chem. Res. 37 (2004) 53–59. doi:10.1021/ar020177t.

[12] J.A. Hawkes, T. Dittmar, C. Patriarca, L. Tranvik, J. Bergquist, Evaluation of the Orbitrap Mass Spectrometer for the Molecular Fingerprinting Analysis of Natural Dissolved Organic Matter, Anal. Chem. 88 (2016) 7698–7704. doi:10.1021/acs.analchem.6b01624.

[13] M. Staš, J. Chudoba, D. Kubička, M. Pospíšil, Chemical Characterization of Pyrolysis Bio-oil: Application of Orbitrap Mass Spectrometry, Energy Fuels. 29 (2015) 3233–3240. doi:10.1021/acs.energyfuels.5b00407.

[14] R. Breitling, A.R. Pitt, M.P. Barrett, Precision mapping of the metabolome, Trends Biotechnol. 24 (2006) 543–548. doi:10.1016/j.tibtech.2006.10.006.

[15] E. Alsbou, B. Helleur, Direct Infusion Mass Spectrometric Analysis of Bio-oil Using ESI-Ion-Trap MS, Energy Fuels. 28 (2014) 578–590. doi:10.1021/ef4018288.

[16] S. Lababidi, W. Schrader, Online normal-phase high-performance liquid chromatography/Fourier transform ion cyclotron resonance mass spectrometry: Effects of different ionization methods on the characterization of highly complex crude oil mixtures, Rapid Commun. Mass Spectrom. 28 (2014) 1345–1352. doi:10.1002/rcm.6907.

[17] D.P. Cole, E.A. Smith, Y.J. Lee, High-Resolution Mass Spectrometric Characterization of Molecules on Biochar from Pyrolysis and Gasification of Switchgrass, Energy Fuels. 26 (2012) 3803–3809. doi:10.1021/ef300356u.
[18] J. Lédé, F. Broust, F.-T. Ndiaye, M. Ferrer, Properties of bio-oils produced by biomass fast pyrolysis in a cyclone reactor, Fuel. 86 (2007) 1800–1810. doi:10.1016/j.fuel.2006.12.024.
[19] A.V. Bridgwater, Review of fast pyrolysis of biomass and product upgrading, Biomass Bioenergy. 38 (2012) 68–94. doi:10.1016/j.biombioe.2011.01.048.
[20] D. Vamvuka, Bio-oil, solid and gaseous biofuels from biomass pyrolysis processes—An overview, Int. J. Energy Res. 35 (2011) 835–862. doi:10.1002/er.1804.
[21] M. Stas, D. Kubicka, J. Chudoba, M. Pospisil, Overview of Analytical Methods Used for Chemical Characterization of Pyrolysis Bio-oil, Energy Fuels. 28 (2014) 385–402. doi:10.1021/ef402047y.
[22] C.M. Michailof, K.G. Kalogiannis, T. Sfetsas, D.T. Patiaka, A.A. Lappas, Advanced analytical techniques for bio-oil characterization, Wiley Interdiscip. Rev. Energy Environ. (2016) n/a-n/a. doi:10.1002/wene.208.
[23] R. Olcese, V. Carré, F. Aubriet, A. Dufour, Selectivity of Bio-oils Catalytic Hydrotreatment Assessed by Petroleomic and GC*GC/MS-FID Analysis, Energy Fuels. 27 (2013) 2135–2145. doi:10.1021/ef302145g.
[24] Y. Bi, G. Wang, Q. Shi, C. Xu, J. Gao, Compositional Changes during Hydrodeoxygenation of Biomass Pyrolysis Oil, Energy Fuels. 28 (2014) 2571–2580. doi:10.1021/ef4024405.
[25] N. Sudasinghe, J.R. Cort, R. Hallen, M. Olarte, A. Schmidt, T. Schaub, Hydrothermal liquefaction oil and hydrotreated product from pine feedstock characterized by heteronuclear two-dimensional NMR spectroscopy and FT-ICR mass spectrometry, Fuel. 137 (2014) 60–69. doi:10.1016/j.fuel.2014.07.069.
[26] P.V. Abdelnur, B.G. Vaz, J.D. Rocha, M.B.B. de Almeida, M.A.G. Teixeira, R.C.L. Pereira, Characterization of Bio-oils from Different Pyrolysis Process Steps and Biomass Using High-Resolution Mass Spectrometry, Energy Fuels. 27 (2013) 6646–6654. doi:10.1021/ef400788v.
[27] N.S. Tessarolo, R.C. Silva, G. Vanini, A. Pinho, W. Romão, E.V.R. de Castro, D.A. Azevedo, Assessing the chemical composition of bio-oils using FT-ICR mass spectrometry and comprehensive two-dimensional gas chromatography with time-of-flight mass spectrometry, Microchem. J. 117 (2014) 68–76. doi:10.1016/j.microc.2014.06.006.
[28] D.P. Cole, E.A. Smith, D. Dalluge, D.M. Wilson, E.A. Heaton, R.C. Brown, Y.J. Lee, Molecular characterization of nitrogen-containing species in switchgrass bio-oils at various harvest times, Fuel. 111 (2013) 718–726. doi:10.1016/j.fuel.2013.04.064.
[29] E.A. Smith, Y.J. Lee, Petroleomic Analysis of Bio-oils from the Fast Pyrolysis of Biomass: Laser Desorption Ionization−Linear Ion Trap−Orbitrap Mass Spectrometry Approach, Energy Fuels. 24 (2010) 5190–5198. doi:10.1021/ef100629a.
[30] I. Miettinen, M. Mäkinen, T. Vilppo, J. Jänis, Compositional Characterization of Phase-Separated Pine Wood Slow Pyrolysis Oil by Negative-Ion Electrospray Ionization Fourier Transform Ion Cyclotron Resonance Mass Spectrometry, Energy Fuels. (2015). doi:10.1021/ef5025966.
[31] J.M. Jarvis, A.M. McKenna, R.N. Hilten, K.C. Das, R.P. Rodgers, A.G. Marshall, Characterization of Pine Pellet and Peanut Hull Pyrolysis Bio-oils by Negative-Ion Electrospray Ionization Fourier Transform Ion Cyclotron Resonance Mass Spectrometry, Energy Fuels. 26 (2012) 3810–3815. doi:10.1021/ef300385f.
[32] Y. Liu, Q. Shi, Y. Zhang, Y. He, K.H. Chung, S. Zhao, C. Xu, Characterization of Red Pine Pyrolysis Bio-oil by Gas Chromatography–Mass Spectrometry and Negative-Ion Electrospray Ionization Fourier Transform Ion Cyclotron Resonance Mass Spectrometry, Energy Fuels. 26 (2012) 4532–4539. doi:10.1021/ef300501t.
[33] J. Hertzog, V. Carré, Y. Le Brech, A. Dufour, F. Aubriet, Toward Controlled Ionization Conditions for ESI-FT-ICR-MS Analysis of Bio-Oils from Lignocellulosic Material, Energy Fuels. 30 (2016) 5729–5739. doi:10.1021/acs.energyfuels.6b00655.
[34] I. Leonardis, S. Chiaberge, T. Fiorani, S. Spera, E. Battistel, A. Bosetti, P. Cesti, S. Reale, F. De Angelis, Characterization of Bio-oil from Hydrothermal Liquefaction of Organic Waste by NMR

Spectroscopy and FTICR Mass Spectrometry, Chemsuschem. 6 (2013) 160–167. doi:10.1002/cssc.201200314.
[35] Y. Le Brech, L. Jia, S. Cissé, G. Mauviel, N. Brosse, A. Dufour, Mechanisms of biomass pyrolysis studied by combining a fixed bed reactor with advanced gas analysis, J. Anal. Appl. Pyrolysis. 117 (2016) 334–346. doi:10.1016/j.jaap.2015.10.013.
[36] S. Schramm, V. Carré, J.-L. Scheffler, F. Aubriet, Analysis of Mainstream and Sidestream Cigarette Smoke Particulate Matter by Laser Desorption Mass Spectrometry, Anal. Chem. 83 (2011) 133–142. doi:10.1021/ac1019842.
[37] Y. Jiang, R.B. Cole, Oligosaccharide analysis using anion attachment in negative mode electrospray mass spectrometry, J. Am. Soc. Mass Spectrom. 16 (2005) 60–70. doi:10.1016/j.jasms.2004.09.006.
[38] A. Le Masle, D. Angot, C. Gouin, A. D'Attoma, J. Ponthus, A. Quignard, S. Heinisch, Development of on-line comprehensive two-dimensional liquid chromatography method for the separation of biomass compounds, J. Chromatogr. A. 1340 (2014) 90–98. doi:10.1016/j.chroma.2014.03.020.
[39] M. Staš, J. Chudoba, M. Auersvald, D. Kubička, S. Conrad, T. Schulzke, M. Pospíšil, Application of orbitrap mass spectrometry for analysis of model bio-oil compounds and fast pyrolysis bio-oils from different biomass sources, J. Anal. Appl. Pyrolysis. (n.d.). doi:10.1016/j.jaap.2017.02.002.
[40] D.M. Osborne, D.C. Podgorski, D.A. Bronk, Q. Roberts, R.E. Sipler, D. Austin, J.S. Bays, W.T. Cooper, Molecular-level characterization of reactive and refractory dissolved natural organic nitrogen compounds by atmospheric pressure photoionization coupled to Fourier transform ion cyclotron resonance mass spectrometry, Rapid Commun. Mass Spectrom. 27 (2013) 851–858. doi:10.1002/rcm.6521.
[41] L.C. Short, S.-S. Cai, J.A. Syage, APPI-MS: Effects of Mobile Phases and VUV Lamps on the Detection of PAH Compounds, J. Am. Soc. Mass Spectrom. 18 (2007) 589–599. doi:10.1016/j.jasms.2006.11.004.
[42] E. Grimsrud, P. Kebarle, Gas-Phase Ion Equilibria Studies of Solvation of Hydrogen-Ion by Methanol, Dimethyl Ether, and Water - Effect of Hydrogen-Bonding, J. Am. Chem. Soc. 95 (1973) 7939–7943. doi:10.1021/ja00805a002.
[43] A. Holle, A. Haase, M. Kayser, J. Höhndorf, Optimizing UV laser focus profiles for improved MALDI performance, J. Mass Spectrom. 41 (2006) 705–716. doi:10.1002/jms.1041.

CAPTION

Table 1: Relative distribution of compound families identified in bio-oil using positive and negative detection mode in ESI, LDI and APPI FT-ICR MS.

Figure 1: Relative intensities of the $C_xH_yO_z$ compounds in (+) and (–) ESI, APPI and LDI FT-ICR MS spectra of wood-derived bio-oil according to the DBE and oxygen atom distributions

Figure 2: Relative intensities of the $C_xH_yO_z$ compounds in wood-derived bio-oil represented on the van Krevelen diagrams according to their H/C and O/C ratios as obtained by (+) and (–) ESI, APPI and LDI FT-ICR MS.

Figure 3: Venn diagrams of $C_xH_yO_z$ compounds in wood-derived bio-oil obtained in (a) positive ion mode and (b) negative ion mode.

Table 1

	# ^{12}C identified compounds	$C_xH_yO_z$	$C_xH_yNO_z$	$C_xH_ySO_z$
ESI (+)	1521	95%	5%	–
ESI (-)	1382	95%	2%	3%
APPI (+)	2778	90%	10%	–
LDI (-)	936	92%	3%	5%
LDI (+) *	415	83%	17%	–
LDI (-) *	1222	97%	3%	–

** 9.4T FT-ICR MS*

Figure 1

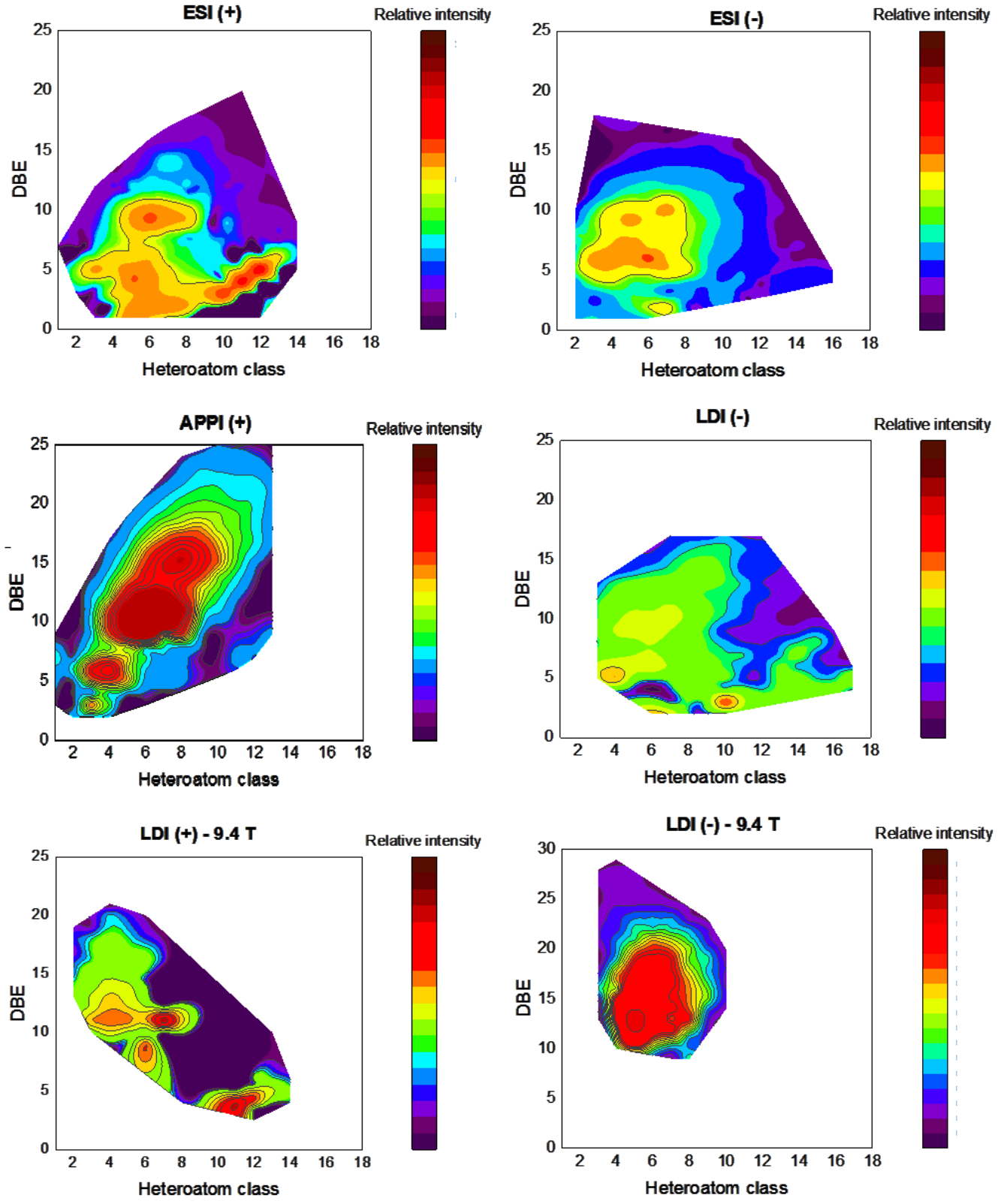

Color for online only

Figure 2

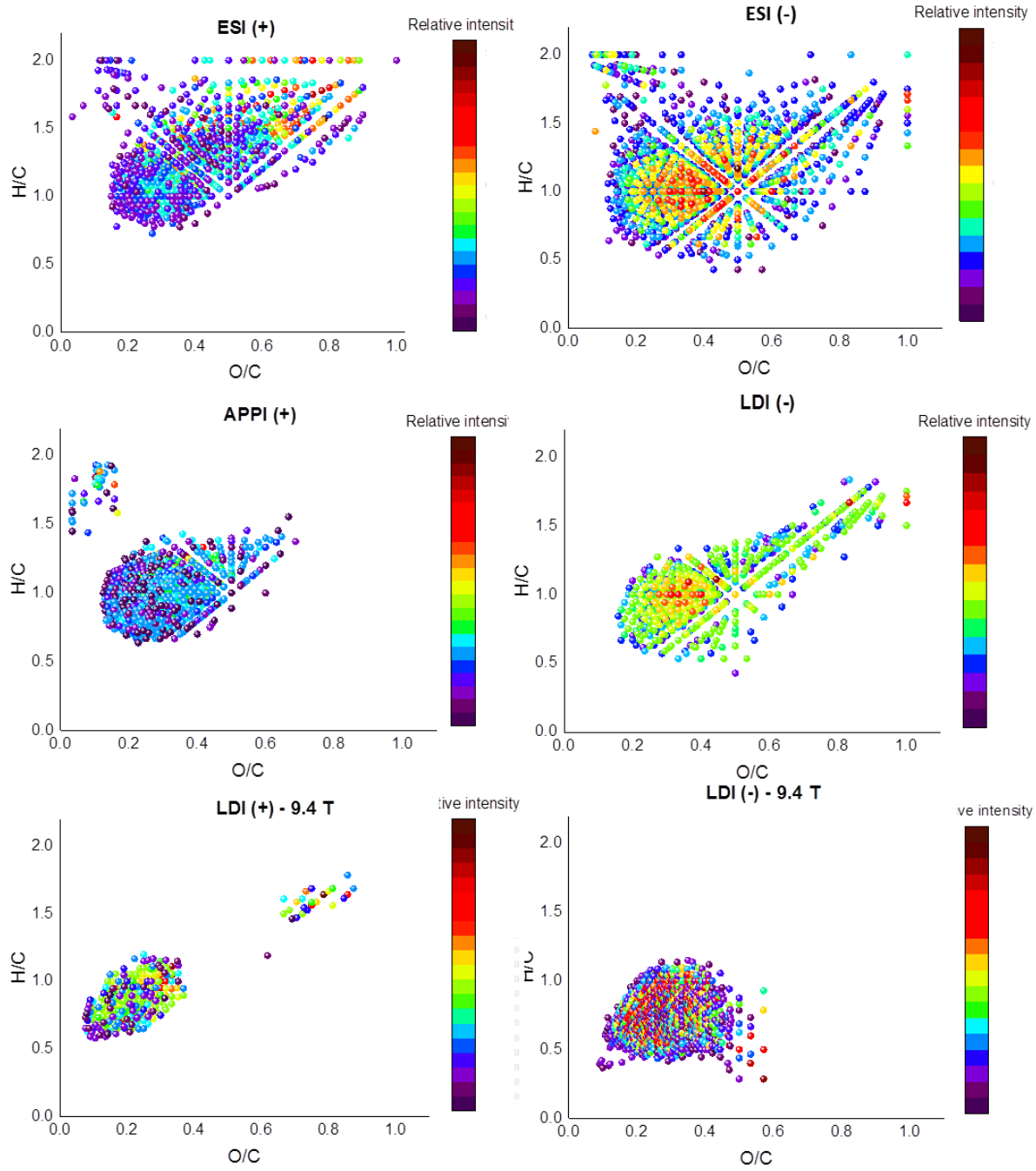

Color for online only

Figure 3

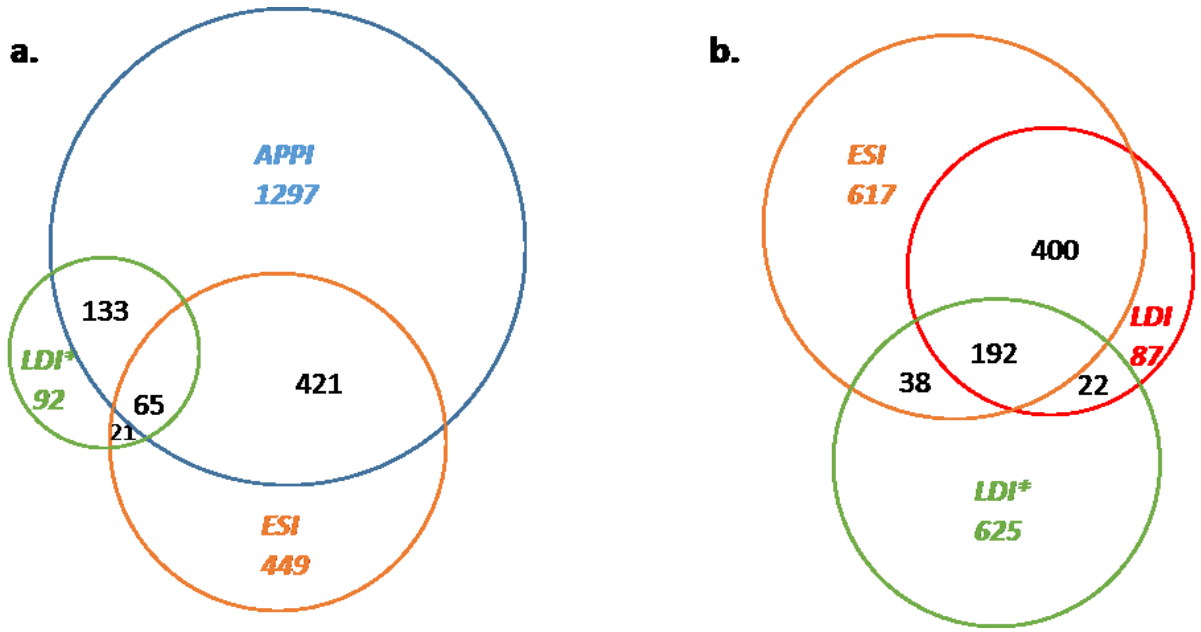

** 9.4T FT-ICR MS*

Color for online only